

AD-A131 393

YIELD SURFACE FOR BARS INCLUDING WARPING RESTRAINT(U)
WEIDLINGER ASSOCIATES NEW YORK R P DADDAZIO ET AL.
01 FEB 82 DNA-TR-81-121 DNA001-81-C-0048

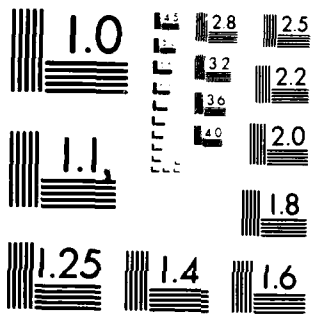
1//

UNCLASSIFIED

F/G 11/4

NL

END
DATE
FILMED
9 83
DTIC



MICROCOPY RESOLUTION TEST CHART
NATIONAL BUREAU OF STANDARDS-1963-A

12

DNA-TR-81-121

ADA 131393

YIELD SURFACE FOR BARS INCLUDING WARPING RESTRAINT

Weidlinger Associates
333 Seventh Avenue
New York, New York 10001

1 February 1982

Technical Report

CONTRACT No. DNA 001-81-C-0048

APPROVED FOR PUBLIC RELEASE;
DISTRIBUTION UNLIMITED.

THIS WORK WAS SPONSORED BY THE DEFENSE NUCLEAR AGENCY
UNDER RDT&E RMSS CODE B344081466 Y99QAXSF00002 H2590D.

DTIC FILE COPY

Prepared for
Director
DEFENSE NUCLEAR AGENCY
Washington, DC 20305

DTIC
ELECTE
AUG 15 1983
S B

83 07 18 045

Destroy this report when it is no longer needed. Do not return to sender.

PLEASE NOTIFY THE DEFENSE NUCLEAR AGENCY,
ATTN: STTI, WASHINGTON, D.C. 20305, IF
YOUR ADDRESS IS INCORRECT, IF YOU WISH TO
BE DELETED FROM THE DISTRIBUTION LIST, OR
IF THE ADDRESSEE IS NO LONGER EMPLOYED BY
YOUR ORGANIZATION.



UNCLASSIFIED

SECURITY CLASSIFICATION OF THIS PAGE (When Data Entered)

REPORT DOCUMENTATION PAGE		READ INSTRUCTIONS BEFORE COMPLETING FORM
1. REPORT NUMBER DNA-TR-81-121	2. GOVT ACCESSION NO. JD 4131 323	3. RECIPIENT'S CATALOG NUMBER
4. TITLE (and Subtitle) YIELD SURFACE FOR BARS INCLUDING WARPING RESTRAINT		5. TYPE OF REPORT & PERIOD COVERED Technical Report
		6. PERFORMING ORG. REPORT NUMBER
7. AUTHOR(s) R.P. Daddazio M.P. Bieniek F.L. DiMaggio		8. CONTRACT OR GRANT NUMBER(s) DNA 001-81-C-0048
9. PERFORMING ORGANIZATION NAME AND ADDRESS Weidlinger Associates 333 Seventh Avenue New York, New York 10001		10. PROGRAM ELEMENT, PROJECT, TASK AREA & WORK UNIT NUMBERS Task Y99QAXSF-00002
11. CONTROLLING OFFICE NAME AND ADDRESS Director Defense Nuclear Agency Washington, D.C. 20305		12. REPORT DATE 1 February 1982
		13. NUMBER OF PAGES 42
14. MONITORING AGENCY NAME & ADDRESS (if different from Controlling Office)		15. SECURITY CLASS. (of this report) UNCLASSIFIED
		15a. DECLASSIFICATION/DOWNGRADING SCHEDULE N/A since UNCLASSIFIED
16. DISTRIBUTION STATEMENT (of this Report) Approved for public release; distribution unlimited.		
17. DISTRIBUTION STATEMENT (of the abstract entered in Block 20, if different from Report)		
18. SUPPLEMENTARY NOTES This work was sponsored by the Defense Nuclear Agency under RDT&E RMSS Code B344081466 Y99QAXSF00002 H2590D.		
19. KEY WORDS (Continue on reverse side if necessary and identify by block number) Plastic Analysis Torsion Yield Surface Thin Walled Open Cross Section Warping Ring Stiffener Bimoment Plastic Properties Yield Mechanism Strucural Analysis		
20. ABSTRACT (Continue on reverse side if necessary and identify by block number) A procedure is described for deriving yield surface equations for thin walled open cross sections for cases in which Saint Venant torsion is small compared to warping torsion. The yield surface equations are expressed in terms of an axial force, bending moments in two planes, and the warping moment or bimoment. Equations are derived for the specific case of a z-section. These equations are shown to satisfy the uniqueness theorem of plastic analysis thereby		

DD FORM 1473
1 JAN 73EDITION OF 1 NOV 68 IS OBSOLETE
S/N 0102-014-6001

UNCLASSIFIED

SECURITY CLASSIFICATION OF THIS PAGE (When Data Entered)

UNCLASSIFIED

SECURITY CLASSIFICATION OF THIS PAGE(When Data Entered)

20. ABSTRACT (Continued)

↙ furnishing the correct yield surface within the limits of validity of the assumptions made, The applicability and accuracy of the proposed equations are indicated.

UNCLASSIFIED

SECURITY CLASSIFICATION OF THIS PAGE(When Data Entered)

TABLE OF CONTENTS

	<u>Page</u>
PREFACE	1
LIST OF ILLUSTRATIONS	3
INTRODUCTION	5
KINEMATICS OF THIN WALLED OPEN CROSS SECTIONS	7
DECOUPLING OF THE MIXED TORSION PROBLEM	9
PLASTIC BEHAVIOR.	11
DETERMINATION OF A LOWER BOUND YIELD SURFACE.	13
DETERMINATION OF UPPER BOUND - YIELD MECHANISMS - UNIQUENESS.	17
ACCURACY AND IMPLEMENTATION OF THE PROPOSED FORMULATION	20
CONCLUSION	21
REFERENCES.	22
NOTATION	24

LIST OF ILLUSTRATIONS

<u>Figure</u>		<u>Page</u>
1	Cross Section Displacements.....	28
2	Stress Components.....	28
3	Stress Resultants....	29
4	Z Stiffened Cylindrical Shell.....	30
5	Assumed Normal Stress Distributions.....	31
6	Z Section.....	31
7	Yield Surface Equations.....	32
8	Yield Surface Equations.....	33
9	Assumed Stress Distribution for Surface Element 1.....	34
10	Assumed Stress Distribution for Surface Element 2.....	34
11	Z Section Yield Surface.....	34
12	Z Section Yield Surface.....	35
13	Z Section Yield Surface.....	36

INTRODUCTION

In recent years, considerable progress has been made in the development of computer programs to perform dynamic, large deflection, elasto-plastic analysis of submarine structures (1, 2, 3). A typical problem of interest is the dynamic elasto-plastic analysis of submerged, stiffened cylinders. Stiffeners on such cylinders are usually thin walled open cross sections such as T, Z, L or flat bar sections.

It is well known that if a section has an enforced center of rotation, (i.e. it is not free to twist about its shear center, as a stiffener welded to a shell is not), there is an increase in the warping resistance of the section to torsion (13, 22). For certain cases, it has been shown that the stresses resulting from resistance to warping can have considerable effect on member response and stability (12, 13, 23). In addition, experiments (7, 8, 19) have clearly indicated that importance of stiffener tripping (lateral-torsional instability) as a critical failure mode for ship structures. Hence, it becomes desirable to consider restrained warping stresses in the development of an elasto-plastic stiffener for inclusion in the analysis of stiffened cylinders.

The inclusion of warping stresses in the elastic response of thin walled open cross sections has been studied by many authors in great detail (13, 14, 22). The plastic response of the section under combined stresses is defined by a yield surface. Following procedures suggested by Hodge (16), Morris and Fenves (19) have determined an approximate lower bound to the exact yield surface for a variety of cross sectional types. This investigation included Saint Venant torsion but neglected warping restraint. Boulton (5), Dinno (9, 10) and Gjelsvik (13) have studied the effect of warping restraint on plastic collapse of thin walled open cross sections, but only for simplified cases in which one or more of the possible stress resultants are zero.

This report presents the formulation of an elasto-plastic thin walled open cross section when the effect of warping torsion is more important than Saint Venant torsion. Equations are developed for the yield surface of a Z-section in terms of four stress resultants, namely the axial force, bending moments in two planes, and the warping moment. These are shown to satisfy both upper and lower bound theorems of plasticity and therefore correspond to exact yield surfaces within the assumptions of thin walled sections.

The development of a yield surface including warping restraint is a necessary first step in the analysis of inelastic stiffener tripping. The equations are currently being incorporated into the computer program EPSA (2), developed at Weidlinger Associates under DNA/ONR sponsorship. This implementation is aimed at extending the modeling capability of EPSA to include stiffener tripping and improving structural response predictions in critical regions of large strain and deformation. This capability will be required in the analysis of a series of plastic range tests on both torpedo (7) and submarine scaled model (8) structures.

KINEMATICS OF THIN WALLED OPEN CROSS SECTIONS

The assumptions made in the formulation of the theory of thin walled beams are that cross sections deform as rigid bodies, and that the shear strain at the middle surface of the section is zero (13, 22).

Referring to Fig. 1, the axial displacement of a point on the middle surface of the bar, $w(s, z)$, may be written as (13),

$$w(s, z) = W(z) - U'(z) x(s) - V'(z) y(s) - \phi'(z) \omega(s) \quad (1)$$

where \bar{n} - s - z are coordinates with \bar{n} normal to, and s following the contour of the middle surface; $U(z)$, $V(z)$, $W(z)$ represent the translation of the center of rotation P in the x - y - z coordinate system; $\phi(z)$ is the rotation of the section about the pole P ; $\omega(s)$ is the warping function defined as

$$\omega(s) = \int_0^s r(s) ds \quad (2)$$

where $r(s)$ is the perpendicular distance from the point P to the point in question on the middle surface. Thickness or secondary warping is neglected in Equation 2.

The first three terms on the right hand side of Equation 1 satisfy Navier's assumption while the last term represents warping.

Stress and Strain Components

The only non-zero stress components are the longitudinal stress, σ_{zz} , and the shearing stress, τ_{zs} , shown in Fig. 2. All stress and strain components normal to the wall are neglected. In addition, all in-plane strains are assumed small. From Eq. 1, the longitudinal strain

is

$$\varepsilon_{zz}(s,z) = W'(z) - U''(z) x(s) - V''(z) y(s) - \phi''(z) \omega(s) \quad (3)$$

If it is desired to extend this formulation to account for geometric nonlinearities, the appropriate nonlinear strain-displacement relations would have to be introduced. This has been done in (6).

Stress Resultants

The strain energy per unit length of the bar, U_s , can be expressed as (13),

$$2U_s = NW' + M_y U'' - M_x V'' + M_\omega \phi'' + T_s \phi' \quad (4)$$

In Eq. 4, the stress resultants N , M_y , and M_x represent the axial force and bending moments about the y-axis and x-axis, respectively, Saint Venant torque is denoted by T_s , and M_ω is the warping moment, or bimoment, and is defined as

$$M_\omega = - \int_A \sigma_{zz} \omega \, dA \quad (5)$$

These stress resultants are shown in Fig. 3.

DECOUPLING OF THE MIXED TORSION PROBLEM

The last two terms of the right hand side of Eq. 4 are the contribution of the warping moment and Saint Venant torsion to the strain energy of the bar. In certain applications, effects of one of these may predominate. In the elastic range, the relative importance of Saint Venant torsion to the warping torsion in straight beams is given by the magnitude of a dimensionless bar parameter, μ_L , defined in (13) as

$$\mu_L = L/d \quad (6)$$

in which L is the span length of the bar and d is a characteristic length defined by

$$d^2 = EI_{\omega\omega}/GJ \quad (7)$$

where E and G denote Young's modulus and the shear modulus and $I_{\omega\omega}$ and J are the warping constant and torsion constant.

It has been shown, (13 , 22), that when μ_L is small (approximately 1) warping torsion is dominant and the Saint Venant torsion term in Eq. 4 may be neglected. If μ_L is large (approximately 20), Saint Venant torsion controls and the term containing the warping moment in Eq. 4 may be dropped.

In the plastic range, the relative importance of these two effects may be estimated by using Eq. 6 with d assumed equal to its elastic value and L taken as an effective length corresponding to plastic deformation patterns of the bar.

Case Study

The preceding discussion on approximations to the mixed torsion problem is applied to a typical problem of interest. Consider the

ring-stiffened cylinder in Fig. 4. A cross section of a typical stiffener is also shown. The value for the warping constant, $I_{\omega\omega}$, for the 2-stiffener with an enforced center of rotation about the line of attachment between the stiffener and the shell is $.0176 \text{ in}^6$ ($4.73 \times 10^6 \text{ mm}^6$). The value of the torsional constant, J , is $.00253 \text{ in}^4$ (1053 mm^4), (14, 15). Using a value for $E/G = 2.6$ for the steel structure, d^2 given by Eq. 7 is 18 in^2 (11610 mm^2).

It has been shown experimentally and analytically in (4, 18) that for cylinders with relatively stiff ring-stiffeners, plastic deformational patterns are characterized by a large number of circumferential waves (typically greater than five). A conservative estimate of an upper bound to the effective length of the ring-stiffener may therefore be taken to be that corresponding to the $n = 5$ deformational mode. The resulting value of μ_L should also be an upper bound. The effective length is then one-tenth of the ring circumference. Using a value of 8.9 in (226 mm) for the length of the stiffener, a value of $\mu_L = 2$ is obtained. With this value of μ_L as an upper bound, Saint Venant torsion may be neglected in Eq. 4, and only the four stress resultants contributing to the axial stress, σ_{zz} , need be considered.

PLASTIC BEHAVIOR

In the formulation of a plastic theory of thin walled bars, the assumption is made that the kinematics describing the plastic behavior of the bar are the same as in the elastic range, (13).

The plastic response of a bar is defined by a yield surface. The assumptions made in the derivation of this surface, in addition to the kinematic ones are the following:

- 1) the material is elastic-perfectly plastic,
- 2) the von Mises yield condition applies,
- 3) shear stresses due to warping are ignored as in plastic beam theory, (20),
- 4) the yield surface is a closed, convex surface and the incremental plastic deformation is directed outward, normal to the surface. With these assumptions, Drucker's hypotheses, (11), are satisfied insuring both uniqueness and stability of plastic response.

The validity of any proposed yield surface may be assessed using the upper and lower bound theorems of plastic analysis, (20). The lower bound theorem states that if a yield surface is derived from a safe and statically admissible stress state it will be enclosed by or coincide with the correct yield surface. The upper bound theorem states that if the states of stress on a yield surface correspond to assumed mechanisms, that yield surface encloses or coincides with the correct yield surface. These theorems may be combined to form a uniqueness theorem which states that a yield surface, derived from a

safe and statically admissible stress state, and corresponding to a kinematically admissible mechanism, is the one correct yield surface.

The yield condition, formulated in terms of normalized stress resultants, involves only those stress resultants which are contained in the expression for the strain energy, (16). Referring to the previous discussion on approximations in the mixed torsion problem, it is assumed that the effects of Saint Venant torsion are negligible. The strain energy of the bar, U_s , of Eq. 4, reduces to

$$2U_s = NW' + M_y U'' - M_x V'' + M_\omega \phi'' \quad (8)$$

Hence, the yield condition may be expressed in terms of the dimensionless parameters

$$n = N/N_p \quad (9a)$$

$$m_x = M_x/M_{xp} \quad (9b)$$

$$m_y = M_y/M_{yp} \quad (9c)$$

$$m_\omega = M_\omega/M_{\omega p} \quad (9d)$$

in which N , M_x , M_y , and M_ω are the previously defined stress resultants shown in Fig. 3 and N_p , M_{xp} , M_{yp} , $M_{\omega p}$ are their fully plastic values. Since shear stresses have been neglected, the von Mises yield condition reduces to

$$\sigma_{zz}^2 = \sigma_y^2 \quad (10)$$

in which σ_y is the yield stress of the material under uniaxial stress.

DETERMINATION OF A LOWER BOUND YIELD SURFACE

It is evident from Eq. 1 that, if warping is considered, Navier's hypothesis is not valid for the cross section as a whole. It is assumed, however, that Navier's hypothesis does hold for each element of the cross section. This implies that there is one neutral axis contained in each element of the cross section.

The equations for the yield surface may be simplified by the following approximations for thin walled sections (19);

- 1) the neutral axis passes perpendicularly through any element of the section, as shown in Fig. 5, or,
- 2) if the neutral axis lies wholly within an element, it is parallel to the long dimension of the element, Fig. 5.

To illustrate the derivation of yield surface equations for a thin walled open cross section including warping stresses, consider the Z-section in Fig. 6. The dimensions of the section which has an enforced center of rotation at P are:

b = width of the flanges;

h = depth of section, center to center of the flanges;

A_f = area of one flange; A_w = area of web;

t = thickness of web and flanges; $c = A_w/A_f = h/b$;

\bar{h} = distance from P to center of top flange where typically $h/\bar{h} \approx 1$.

The fully plastic stress resultants are found to be:

$$N_p = \sigma_y A_f (2 + c) \quad (11a)$$

$$M_{xp} = \frac{1}{4} \sigma_y A_f h (4 + c) \quad (11b)$$

$$M_{yp} = \sigma_y A_f b \quad (11c)$$

$$M_{wp} = \frac{1}{2} \sigma_y A_f b \bar{h} \quad (11d)$$

In general, a yield surface has several elements each related to generic neutral axis positions. The approximations regarding neutral axis location within an element allow a reduction in the number of surface elements comprising the yield surface of a Z-section to four. They are shown in Fig. 7. However, since the section is not symmetric, four complementary cases are necessary for complete determination of the yield surface. In these complementary cases, indicated in Fig. 8, the generic neutral axis locations of Fig. 7 are unchanged but the sign of the yield stress is reversed.

The stress resultants corresponding to the stress distribution of Fig. 9 are:

$$N = \sigma_y A_f (2 + c - 2(\beta + \gamma c + \alpha)) \quad (12a)$$

$$M_x = \sigma_y A_f h (\gamma c (\gamma - 1) - \alpha + \beta) \quad (12b)$$

$$M_y = \sigma_y A_f b (\beta^2 - 2\beta + \alpha^2) \quad (12c)$$

$$M_\omega = \frac{1}{2} \sigma_y A_f b \bar{h} (1 - 2\alpha^2) \quad (12d)$$

in which α , β , and γ are dimensionless parameters that define the neutral axis location in each element of the cross section.

The corresponding normalized stress resultants, found by substituting Eqs. 12 and 11 into Eqs. 9, are:

$$n = 1 - \frac{2(\beta + \gamma c + \alpha)}{2 + c} \quad (13a)$$

$$m_x = \frac{4}{4+c} (\gamma c (\gamma - 1) - \alpha + \beta) \quad (13b)$$

$$m_y = \beta^2 - 2\beta + \alpha^2 \quad (13c)$$

$$m_\omega = 1 - 2\alpha^2 \quad (13d)$$

Eliminating the parameters α , β , and γ from Eqs. 13, the equation of the element of the yield surface for this case is obtained as

$$\left[\frac{2+c}{2} (1-n) - \left(1 - \sqrt{\frac{1}{2} (1+m_\omega) + m_y} + \sqrt{\frac{1}{2} (1-m_\omega)} \right) \right] \\ \times \left[\frac{2+c}{2c} (1-n) - \frac{1}{c} \left(1 - \sqrt{\frac{1}{2} (1-m_\omega) + m_y} + \sqrt{\frac{1}{2} (1-m_\omega)} \right) - 1 \right] \quad (14) \\ + 1 - \sqrt{\frac{1}{2} (1+m_\omega) + m_y} - \sqrt{\frac{1}{2} (1-m_\omega)} - \left(\frac{4+c}{4} \right) m_x = 0$$

Consider the stress distribution shown in Fig. 10. In this case, a neutral axis lies within the bottom flange. The values of n and m_x are insensitive to the angle θ since it is necessarily small. The normalized warping moment, m_ω , is independent of θ , and the bending moment about the y -axis, m_y , is an unknown function of θ and hence indeterminate. The normalized stress resultants are:

$$n = \frac{c + 2(-1 + \beta + \alpha)}{2 + c} \quad (15a)$$

$$m_x = \frac{4(\beta - \alpha)}{4 + c} \quad (15b)$$

$$m_y = \text{indeterminate} \quad (15c)$$

$$m_\omega = 1 - 2\alpha^2 \quad (15d)$$

The equation for this element of the yield surface, obtained from Eqs. 15, is independent of m_y and may be written

$$(2 + c) n + \frac{4 + c}{2} m_x + \sqrt{8(1 - m_\omega)} + c - 2 = 0 \quad (16)$$

Similarly, equations for the other elements were found. They are shown in tabular form in Figs. 7 and 8. The yield surface constructed from the various surface elements is illustrated in Fig. 11 for the Z -stiffener of Fig. 4. A two dimensional section in the $n - m_x$ plane is shown for $m_y = m_\omega = 0$. The range of applicability of each surface

element is indicated on the figure. Isometric plots of the yield surface are shown in Figs. 12 and 13 for $m_y = 0$ and $m_x = 0$, respectively.

DETERMINATION OF UPPER BOUND - YIELD MECHANISMS - UNIQUENESS

The state of stress in the bar may be expressed in terms of the stress resultants, which may be considered components of a matrix denoted by {Q}:

$$\{Q\} = \{ N, M_y, M_x, M_\omega \} \quad (17)$$

The corresponding matrix of bar strains, {q}, is

$$\{q\} = \{ W', U'', -V'', \phi'' \} \quad (18)$$

The yield surface is a function of the stress resultants such that, at yield,

$$F(N, M_y, M_x, M_\omega) = 0 \quad (19)$$

It has been assumed that the incremental plastic strain is directed outward, normal to the yield surface. This associated flow rule may be stated as

$$\delta q_i = \lambda \frac{\partial F}{\partial Q_i} \quad (20)$$

in which λ is an arbitrary positive proportionality factor and δq_i denotes a component of incremental plastic strain.

From Eq. 20 it follows that the strain increments corresponding to stress points on the yield surface satisfy

$$\frac{\delta q_i}{\delta q_j} = - \frac{\partial Q_j}{\partial Q_i} \quad (21)$$

in which the derivatives on the right hand side are obtained from Eq. 19 .

To illustrate the determination of such strain increment rates, consider, e.g., the lower bound stress distribution of Fig. 10. The yield surface equation for this stress state is given by Eq. 16.

The ratios of the components of the plastic strain increments follow from Eqs. 11, 16, and 21. They are

$$-\frac{\delta V''}{\delta W'} = -\frac{\partial N}{\partial M_x} = \frac{2}{cb} \quad (22a)$$

$$\frac{\delta \phi''}{\delta W'} = -\frac{\partial N}{\partial M_\omega} = -\frac{2}{h\alpha b} \quad (22b)$$

$$\frac{\delta U''}{\delta W'} = -\frac{\partial N}{\partial M_y} = 0 \quad (22c)$$

Yield mechanisms may be determined solely from kinematic considerations. Following Eq. 3, the incremental plastic strain may be written as

$$\delta \epsilon_{zz} = -\delta W' \left(-1 + \frac{\delta U''}{\delta W'} x + \frac{\delta V''}{\delta W'} y + \frac{\delta \phi''}{\delta W'} \omega \right) \quad (23)$$

At a neutral axis location in an element of the cross section, the axial strain, ϵ_{zz} , and hence, $\delta \epsilon_{zz}$, are zero. The neutral axis locations for each surface element are known and indicated in Figs. 7 and 8. Therefore, the components of the yield mechanism may be determined.

Again, consider the stress distribution of Fig. 10. The neutral axis locations and hence the positions at which Eq. 23 equals zero are shown in Table 1. Substitution of the conditions specified in Table 1 into Eq. 23 gives the components of the yield mechanism as follows:

$$-\frac{\delta V''}{\delta W'} = \frac{2}{cb} \quad (24a)$$

$$\frac{\delta \phi''}{\delta W'} = -\frac{2}{h\alpha b} \quad (24b)$$

$$\frac{\delta U''}{\delta W'} = 0 \quad (24c)$$

Comparison of Eqs. 22 and 24 shows that the stress state on this element of the lower bound yield surface corresponds to a yield mechanism. Thus, the uniqueness theorem of plastic analysis is satisfied and the yield surface element, given by Eq. 16, is the correct one.

In a similar manner, the uniqueness theorem can be shown to be satisfied for the remaining surface elements of Figs. 7 and 8. Hence, the complete yield surface, defined by the individual surface elements, is the exact yield surface. The yield mechanisms, derived from kinematics, for each surface element are listed in Table 2.

ACCURACY AND IMPLEMENTATION OF THE PROPOSED FORMULATION

The accuracy of the proposed formulation rests on two approximations. The first involves the elimination of Saint Venant torsion from the yield condition. The second involves assumptions on neutral axis location within the elements of the cross section.

Referring to the earlier discussion on approximations to the mixed torsion problem, it is evident that as the importance of Saint Venant torsion increases, the proposed formulation will be increasingly in error.

The assumption that a neutral axis passes perpendicularly through an element of the cross section leads to artificial ridges in the yield surface. These ridges lie outside the correct yield surface. This approximation was discussed in detail in (19), and has been shown to be negligible in elasto-plastic analysis of thin walled sections.

The technique used in the development of the yield surface for a Z-section including warping stresses can be applied to any thin-walled open cross section. Other common types used as ring-stiffeners for cylindrical shells are T and L sections.

The proposed yield surface equations are suitable for incorporation into the existing nonlinear, elasto-plastic finite element program, EPSA (2). The present stiffener formulation in the code accounts for plastic response in terms of only two stress resultants, namely the axial force and bending moment about the strong axis of the stiffener. The proposed formulation will extend the structural modeling capability for the class of problems such as that shown

in Fig. 4, and lead to an increase in the accuracy of structural response predictions, especially in regions of large plastic strain and deformation.

CONCLUSION

A procedure has been described for deriving yield surface equations for thin-walled open cross sections with an enforced center of rotation for cases in which Saint Venant torsion is small compared to warping torsion. Equations have been derived for the specific case of a Z-section. These equations have been shown to satisfy the uniqueness theorem of plastic analysis thereby furnishing the correct yield surface within the limits of validity of the assumptions made. The applicability and accuracy of the proposed equations are indicated.

REFERENCES

- (1) Almroth, B.O., Brogan, F.A., and Stanley, G.M., "Structural Analysis of General Shells, Volume II, User Instructions for STAGSC," LMSC-D633873, Lockheed Palo Alto Research Laboratory, Palo Alto, California, January 1979.
- (2) Atkatsh, R., and Daddazio, R.P., "Dynamic Elasto-Plastic Response of Shells in an Acoustic Medium User's Manual for the EPSA Code," Technical Report No. 27, ONR Contract No. N00014-78-C-0820, Weidlinger Associates, New York, New York, March 1980.
- (3) Bathe, K.J., "ADINA - A Finite Element Program for Automatic Dynamic Incremental Nonlinear Analysis," Rep. No. 82448-1, Massachusetts Institute of Technology, Cambridge, Massachusetts, September 1975, (rev. Dec. 1978).
- (4) Boichot, L. and Reynolds, T.E., "Inelastic Buckling Tests of Ring-Stiffened Cylinders under Hydrostatic Pressure," David Taylor Model Basin, Washington, D.C., Report 1992, 1965.
- (5) Boulton, N.S., "Plastic Twisting and Bending of an I-Beam in which the Warp is Restricted," Int. J. Mech. Sci., Vol. 4, pp. 491-502, Pergamon Press, 1964.
- (6) Connor, J.J., "Analysis of Structural Member Systems," The Ronald Press Company, New York, 1976.
- (7) Daddazio, R., Atkatsh, R., Baron, M.L. and Bieniek, M.P., "Dynamic Elasto-Plastic Response of Mark 37 Torpedo Afterbodies, EPSA Code Comparisons with Experimental Data (U)," Technical Report, Confidential, Defense Nuclear Agency, Contract No. DNA001-79-C-0078, Weidlinger Associates, New York, New York, January 1980.
- (8) Daddazio, R., Atkatsh, R., Baron, M.L. and Bieniek, M.P., "Intermediate Scale Models Subjected to Simulated Nuclear Loading - EPSA Code Comparisons with ISM-A4 Experimental Data and Implications of the ISM-A3/A4 Test Series (U)," Technical Report, Confidential, Defense Nuclear Agency, Contract No. DNA001-79-C-0078, Weidlinger Associates, New York, New York, January 1981.
- (9) Dinno, K.S., and Gill, S.S., "The Plastic Torsion of I-Sections with Warping Restraint," Int. J. Mech. Sci., Vol. 6, pp. 27-43, Pergamon Press, 1964.
- (10) Dinno, K.S., and Merchant, W., "A Procedure for Calculating the Plastic Collapse of I-Sections under Bending and Torsion," The Structural Engineer, Vol. 43, No. 7, July, 1965, pp. 219-221.

- (11) Drucker, D., "On Uniqueness in the Theory of Plasticity," Q. Appl. Math., Vol. 14, pp. 35-42, 1956.
- (12) Ettouney, M.M., and Kirby, J.B., "Warping Restraint in Three-Dimensional Frames," Journal of the Structural Division, ASCE, Vol. 107, No. St. 8, Proc. Paper 16475, August, 1981, pp. 1643-1656.
- (13) Gjelsvik, A., "The Theory of Thin Walled Bars," John Wiley & Sons, Inc., New York, New York, 1981.
- (14) Heins, C.P., "Bending and Torsional Design in Structural Members," Lexington Books, Lexington, Massachusetts, 1975.
- (15) Heins, C.P., and Wang, R.C., "Torsional Properties of Open Cross Sections," Computers & Structures, Vol. 9, pp. 495-500, Pergamon Press, 1978.
- (16) Hodge, P., "Plastic Analysis of Structures," McGraw-Hill Book Company, Inc., New York, 1959.
- (17) Hodge, P.G. and Sankaranaraya, R., "The Determination of Safe Loads of Beams Subjected to Combined Twisting and Biaxial Bending Moments," Journal of Applied Mechanics., Vol. 26, Trans. ASME, Series E, Number 3, September, 1959, pp. 442-447.
- (18) Lee, L., "General Elastic-Plastic Instability of Ring-Stiffened Cylindrical Shells Under External Pressure," Technical Report No. SM156, ONR Contract No. N00014-67-A-0242-006, University of Notre Dame, Notre Dame, Indiana, February 1973.
- (19) Morris, G.A., and Fenves, S.J., "Approximate Yield Surface Equations," Journal of the Engineering Mechanics Division, ASCE, Vol. 95, No. EM 4, Proc. Paper 6741, August, 1969, pp. 937-954.
- (20) Neal, B.G., "The Plastic Methods of Structural Analysis," John Wiley & Sons, Inc., New York, 1963.
- (21) Smith, C.S., "Compressive Strength of Welded Steel Ship Grillages," Journal of the Royal Institute of Naval Architects, No. 4 (Oct 1975).
- (22) Vlasov, V.A., "Thin Walled Elastic Beams," translated from Russian, published for the National Science Foundation, Washington, D.C., and the U.S. Department of Commerce by the Israel Program for Scientific Translations, Jerusalem, 1961.
- (23) Yoo, C.H., "Bimoment Contribution to Stability of Thin-Walled Assemblages," Computers & Structures, Vol. 11, pp. 465-471, Pergamon Press, 1980.

NOTATION

The following symbols are used in this paper:

A_f	=	cross sectional area of flange;
b	=	width of flange;
c	=	ratio of area of web to area of flange;
d	=	characteristic length;
E	=	Young's modulus;
F	=	function defining yield surface
G	=	shear modulus
h	=	depth of section center to center of flanges;
\bar{h}	=	distance from pole to center of top flange;
I_{ω}	=	warping constant;
J	=	torsion constant;
L	=	length of bar;
M_x	=	bending moment about x-axis;
m_x	=	normalized bending moment about x-axis;
M_{xp}	=	fully plastic bending moment about x-axis;
M_y	=	bending moment about y-axis;
m_y	=	normalized bending moment about y-axis;
M_{yp}	=	fully plastic bending moment about y-axis;
M_{ω}	=	warping moment;
m_{ω}	=	normalized warping moment;
$M_{\omega p}$	=	fully plastic warping moment;
N	=	axial force;
n	=	normalized axial force;
N_p	=	fully plastic axial force;
$\bar{n}-s-z$	=	coordinate system defined at middle surface of cross section;
P	=	pole or center of rotation;
Q	=	matrix of stress resultants;
q	=	matrix of bar strains;
r	=	perpendicular distance from pole to point on middle surface of section;
T_s	=	Saint Venant torque;
t	=	thickness of wall of cross section
$U, V, W,$	=	rigid body displacement of pole in the x, y, z, directions;
U_s	=	strain energy per unit length of bar;
w	=	axial displacement of point on the middle surface of the cross section
x, y, z	=	cartesian coordinates;
α, β, γ	=	dimensionless parameters locating neutral axis in cross section;
δq_i	=	increment of plastic bar strain;

ϵ_{zz} = axial strain in section;
 θ = orientation of neutral axis in element of cross section;
 λ = positive constant;
 λ_L = dimensionless bar parameter
 σ_y = yield stress of material;
 σ_{zz} = axial stress in section;
 τ_{zs} = shear stress in section
 ϕ = rotation of cross section about pole;
 w = contour warping function

Superscript

' = differentiation with respect to z-axis

TABLE 1 - LOCATION OF NEUTRAL AXES FOR SURFACE ELEMENT 2

ELEMENT	x	y	w
TOP FLANGE	xb	$\frac{1}{2} h$	$-h\alpha b$
WEB	0	$-\frac{1}{2} h$	0
BOTTOM FLANGE	$-b \leq x \leq 0$	$-\frac{1}{2} h$	0

TABLE 2 - YIELD MECHANISMS

SURFACE ELEMENT	$\delta W' / \delta \phi''$	$\delta U'' / \delta \phi''$	$-\delta V'' / \delta \phi''$
1	$\frac{\alpha(1-\beta)(1-2\gamma)hb}{2[\alpha+\gamma(1-\beta-\alpha)]}$	$\frac{\alpha(1-\gamma)h}{[\alpha+\gamma(1-\beta-\alpha)]}$	$\frac{-\beta(1-\alpha)b}{[\beta-\gamma(1-\beta-\alpha)]}$
2	$-\frac{1}{2} h\alpha b$	0	$-\alpha b$
3	$-\frac{1}{2} \beta hb$	h	βb
4	0	h	0
1a	$\frac{\beta(1-\alpha)(2\gamma-1)hb}{2[\beta-\gamma(1-\beta-\alpha)]}$	$\frac{-\gamma(1-\alpha)h}{[\beta-\gamma(1+\beta-\alpha)]}$	$\frac{-\alpha(1-\beta)b}{[\alpha+\gamma(1-\beta-\alpha)]}$
2a	$-\frac{1}{2} h(1-\alpha)b$	0	$-(1-\alpha)b$
3a	$-\frac{1}{2} h(1-\beta)b$	h	$(1-\beta)b$
4a	0	h	0

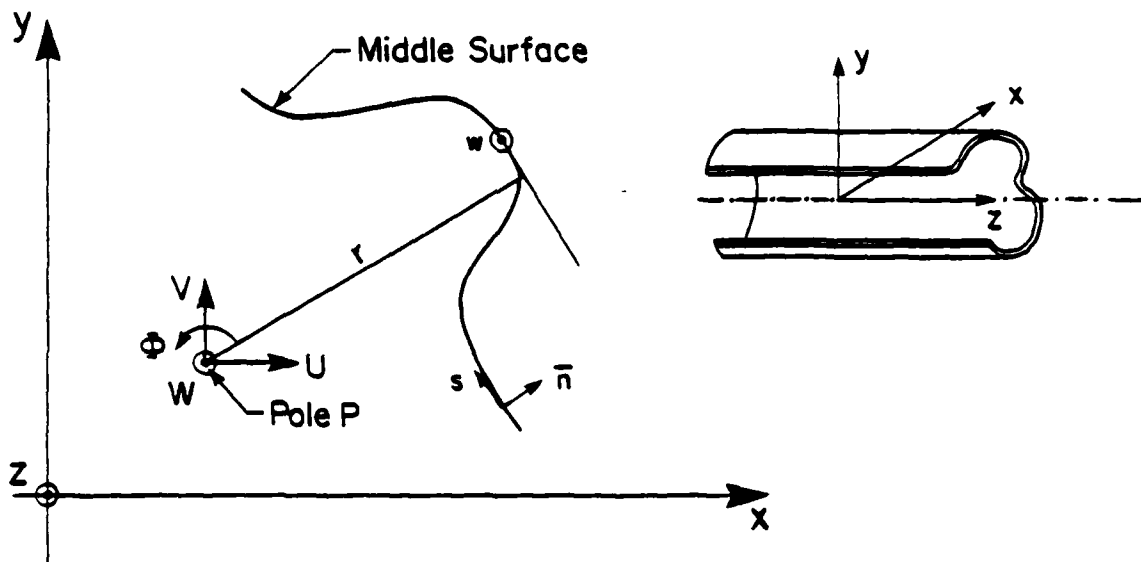


FIG.1 CROSS SECTION DISPLACEMENTS

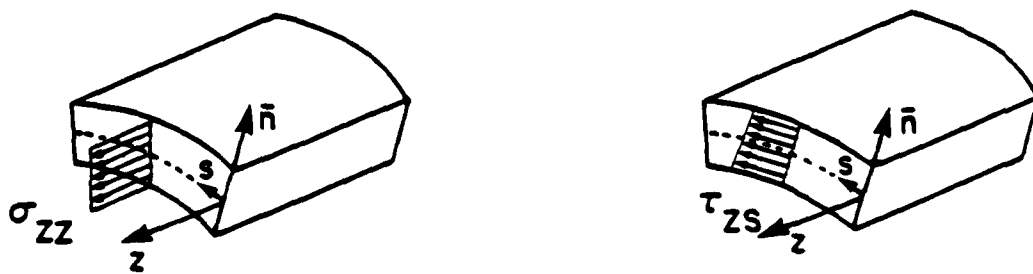


FIG.2 STRESS COMPONENTS

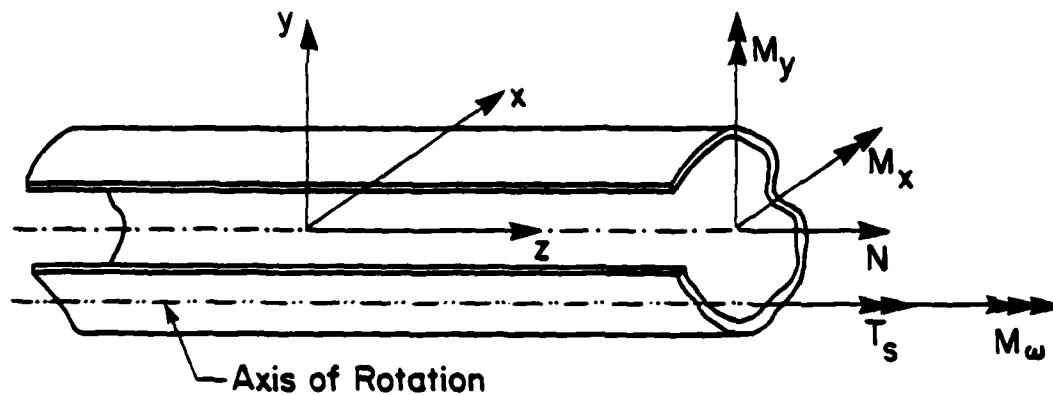


FIG. 3 STRESS RESULTANTS

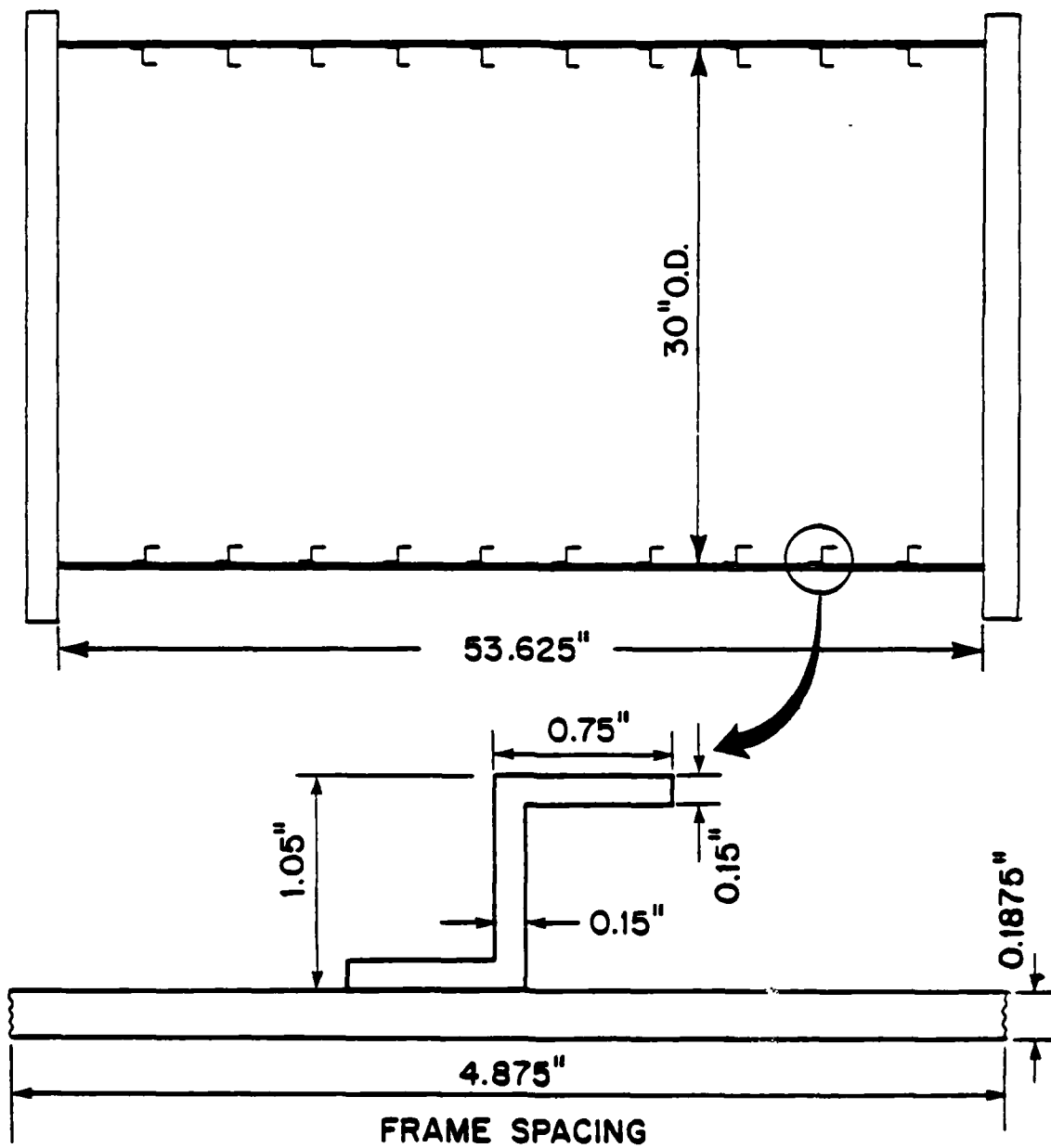


FIG. 4 Z STIFFENED CYLINDRICAL SHELL (1in = 25.4 mm)

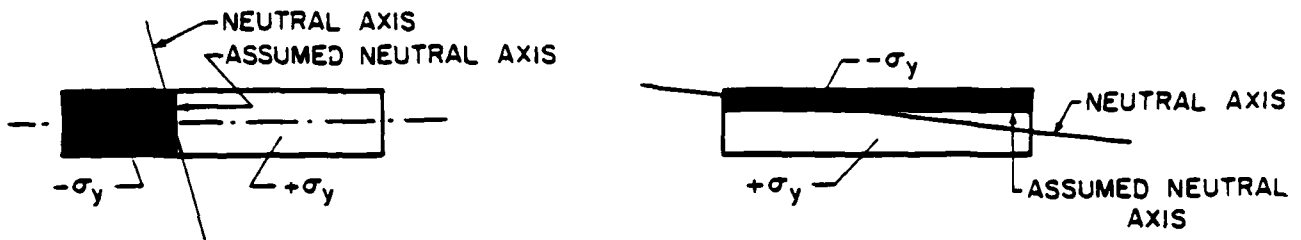


FIG. 5 ASSUMED NORMAL STRESS DISTRIBUTIONS

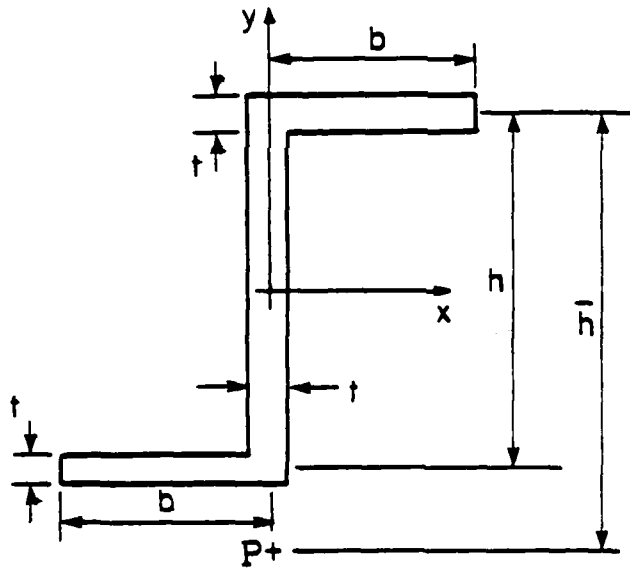


FIG. 6 Z SECTION

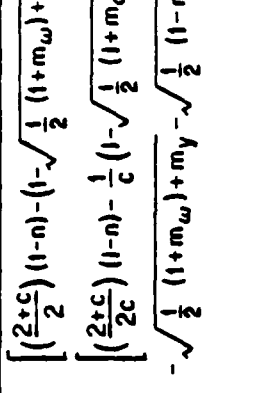
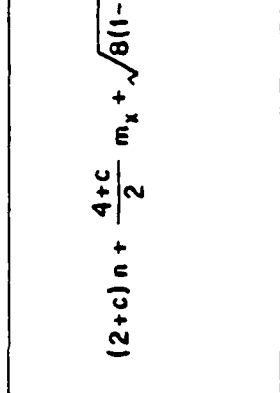
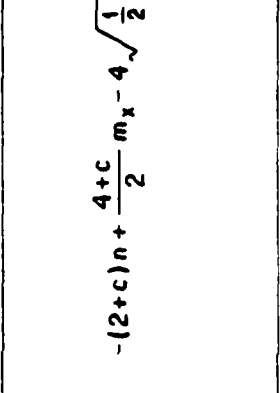
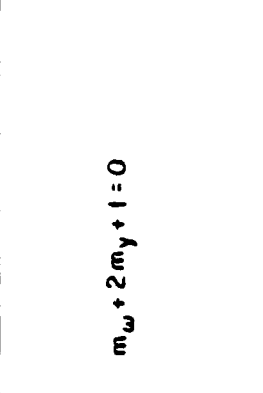
SURFACE ELEMENT	NEUTRAL AXES LOCATION	NORMALIZED STRESS RESULTANTS	YIELD SURFACE EQUATIONS
1		$n = 1 - \frac{2(\beta + \gamma c + a)}{2 + c}$ $m_x = \frac{4}{4+c} \left[\gamma c (\gamma - 1) - a + \beta \right]$ $m_y = \beta^2 - 2\beta + a^2$ $m_\omega = 1 - 2a^2$	$\left[\frac{2+c}{2} (1-n) - \left(1 - \sqrt{\frac{1}{2} (1+m_\omega)} + m_y + \sqrt{\frac{1}{2} (1-m_\omega)} \right) \right] \cdot$ $\left[\frac{2+c}{2c} (1-n) - \frac{1}{c} \left(1 - \sqrt{\frac{1}{2} (1+m_\omega)} + m_y + \sqrt{\frac{1}{2} (1-m_\omega)} \right) - 1 \right] + 1$ $- \sqrt{\frac{1}{2} (1+m_\omega)} + m_y - \sqrt{\frac{1}{2} (1-m_\omega)} - \left(\frac{4+c}{4} \right) m_x = 0$
2		$n = -\frac{c+2(-1+\beta+a)}{2+c}$ $m_x = \frac{4(\beta-a)}{4+c}$ $m_y = \text{indeterminate}$ $m_\omega = 1 - 2a^2$	$(2+c)n + \frac{4+c}{2} m_x + \sqrt{8(1-m_\omega)} + c - 2 = 0$
3		$n = -\frac{c+2(-1+\beta+a)}{2+c}$ $m_x = \frac{4(\beta-a)}{4+c}$ $m_y = \text{indeterminate}$ $m_\omega = \text{indeterminate}$ $\beta = \sqrt{\frac{1}{2} (1-m_\omega)} - m_y$	$-(2+c)n + \frac{4+c}{2} m_x - 4 \sqrt{\frac{1}{2} (1-m_\omega)} - m_y - c + 2 = 0$
4		$n = \text{indeterminate}$ $m_x = \text{indeterminate}$ $m_y = a^2 - 1$ $m_\omega = 1 - 2a^2$	$m_\omega + 2m_y + 1 = 0$ <div style="border: 1px solid black; padding: 5px; width: fit-content; margin: 10px auto;"> <div style="display: flex; justify-content: space-around; width: 100%;"> <div style="border: 1px solid black; width: 15px; height: 10px; background-color: white;"></div> <div style="border: 1px solid black; width: 15px; height: 10px; background-color: black;"></div> </div> <div style="display: flex; justify-content: space-around; width: 100%; margin-top: 5px;"> +σ_y -σ_y </div> </div>

FIG. 7 YIELD SURFACE EQUATIONS

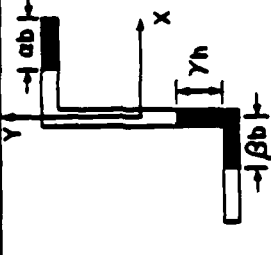
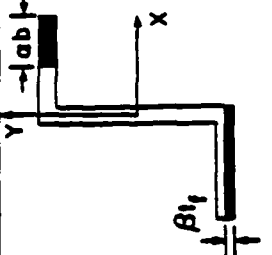
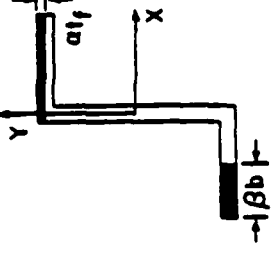
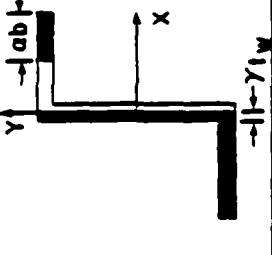
SURFACE ELEMENT	NEUTRAL AXES LOCATION	NORMALIZED STRESS RESULTANTS	YIELD SURFACE EQUATIONS
10		$n = 1 - \frac{2(\beta + \gamma + a)}{2 + c}$ $m_x = \frac{4}{4 + c} \left[\gamma c (1 - \gamma) - a + \beta \right]$ $m_y = -a^2 + 2a - \beta^2$ $m_\omega = 1 - 2a(2 - a)$	$\left[\left(\frac{2+c}{2} \right) (1-n) - \left(\sqrt{\frac{1}{2} (1-m_\omega)} - m_y + 1 \pm \sqrt{\frac{1}{2} (1+m_\omega)} \right) \right] +$ $\left[\left(\frac{2+c}{2c} \right) (1-n) - \frac{1}{c} \left(\sqrt{\frac{1}{2} (1-m_\omega)} - m_y + 1 \pm \sqrt{\frac{1}{2} (1+m_\omega)} \right) - 1 \right] +$ $\sqrt{\frac{1}{2} (1-m_\omega)} - m_y - 1 + \sqrt{\frac{1}{2} (1+m_\omega)} - \left(\frac{4+c}{4} \right) m_x = 0$
20		$n = 1 - \frac{2(\beta + a)}{2 + c}$ $m_x = \frac{4}{4 + c} (\beta - a)$ $m_y = \text{indeterminate}$ $m_\omega = 1 - 2a(2 - a)$	$(2+c)n + \frac{4+c}{2} m_x - \sqrt{8(1+m_\omega)} - c + 2 = 0$
30		$n = 1 - \frac{2(\beta + a)}{2 + c}$ $m_x = \frac{4}{4 + c} (\beta - a)$ $m_y = \text{indeterminate}$ $m_\omega = \text{indeterminate}$ $\beta = 1 - \sqrt{\frac{1}{2} (1+m_\omega)} + m_y$	$-(2+c)n + \frac{4+c}{2} m_x + 4 \sqrt{\frac{1}{2} (1+m_\omega)} + m_y + c - 2 = 0$
40		$n = \text{indeterminate}$ $m_x = \text{indeterminate}$ $m_y = -a^2 + 2a - 1$ $m_\omega = 1 - 2a(2 - a)$	$m_\omega + 2m_y - 1 = 0$ <div style="border: 1px solid black; padding: 5px; width: fit-content; margin: 10px auto;"> <div style="display: flex; justify-content: space-around; align-items: center;"> <div style="border: 1px solid black; width: 15px; height: 10px; background-color: white;"></div> <div style="text-align: center;">+σ_y</div> </div> <div style="display: flex; justify-content: space-around; align-items: center;"> <div style="border: 1px solid black; width: 15px; height: 10px; background-color: black;"></div> <div style="text-align: center;">-σ_y</div> </div> </div>

FIG. 8 YIELD SURFACE EQUATIONS

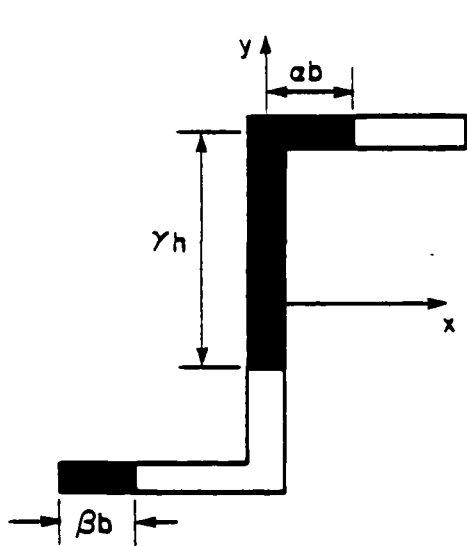


FIG. 9 ASSUMED STRESS DISTRIBUTION FOR SURFACE ELEMENT 1

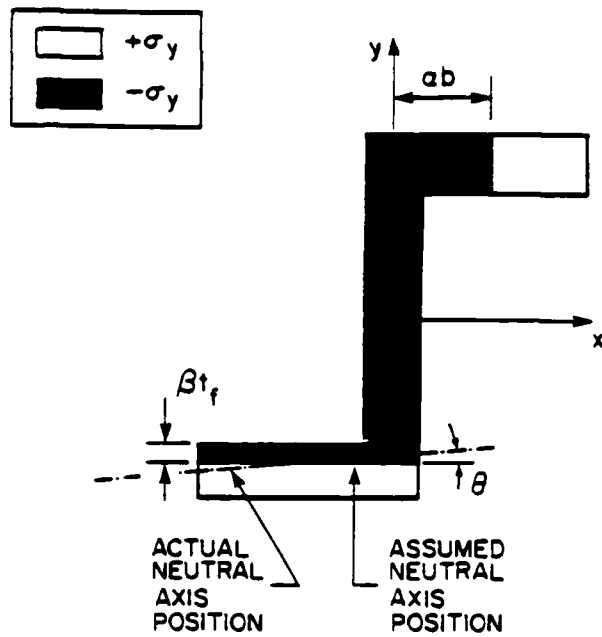


FIG.10 ASSUMED STRESS DISTRIBUTION FOR SURFACE ELEMENT 2

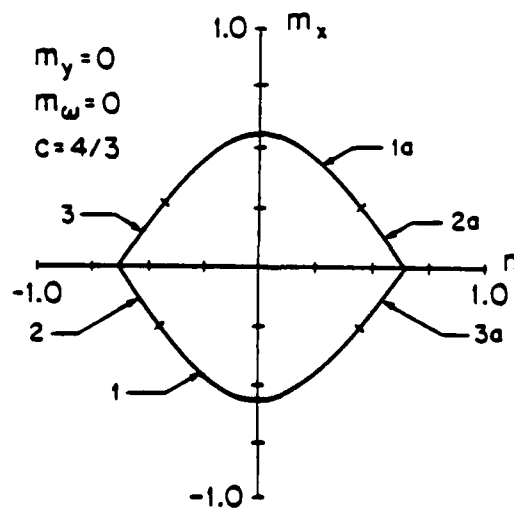


FIG.11 Z SECTION YIELD SURFACE

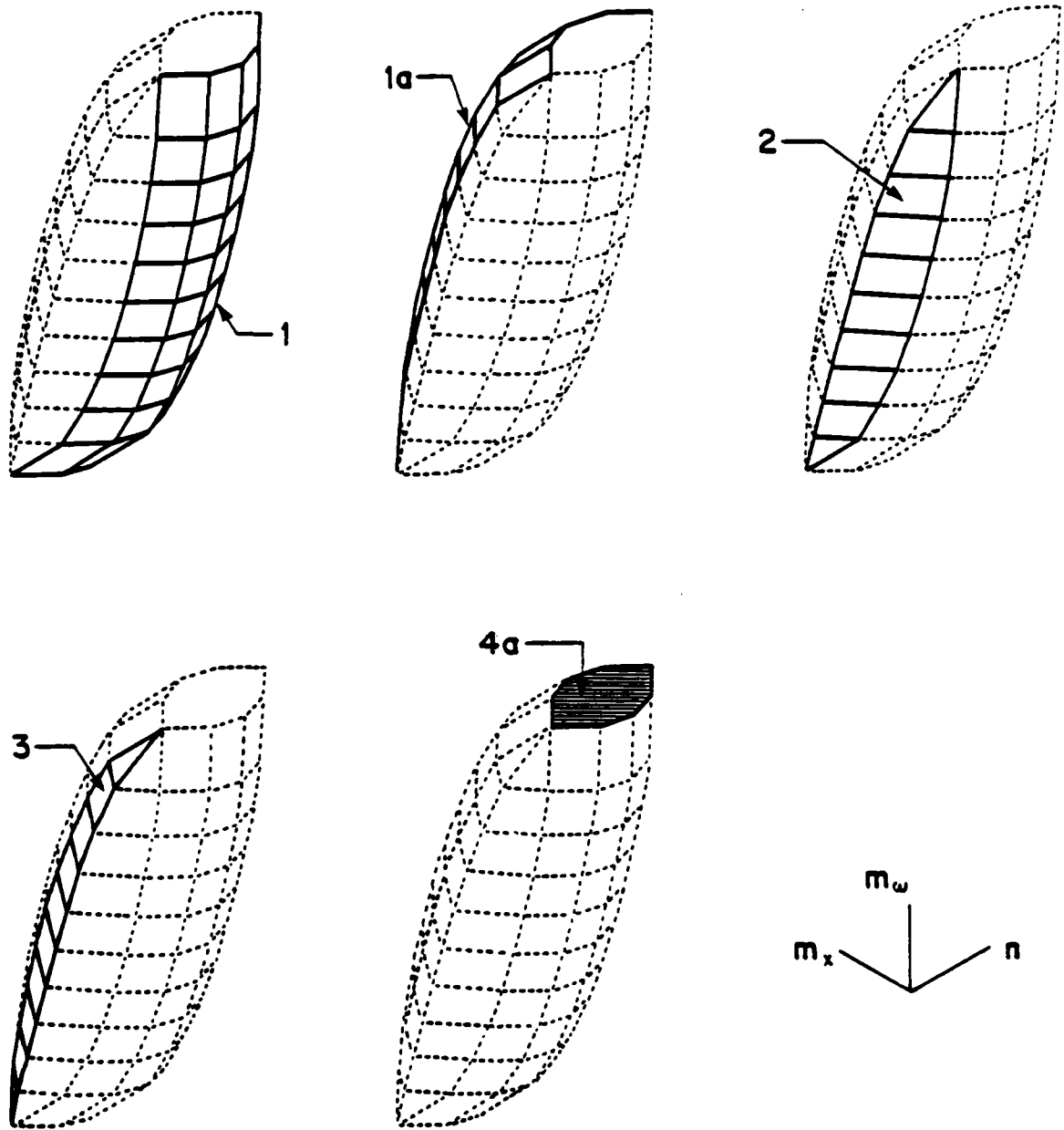


FIG. 12 Z SECTION YIELD SURFACE - $m_y=0$

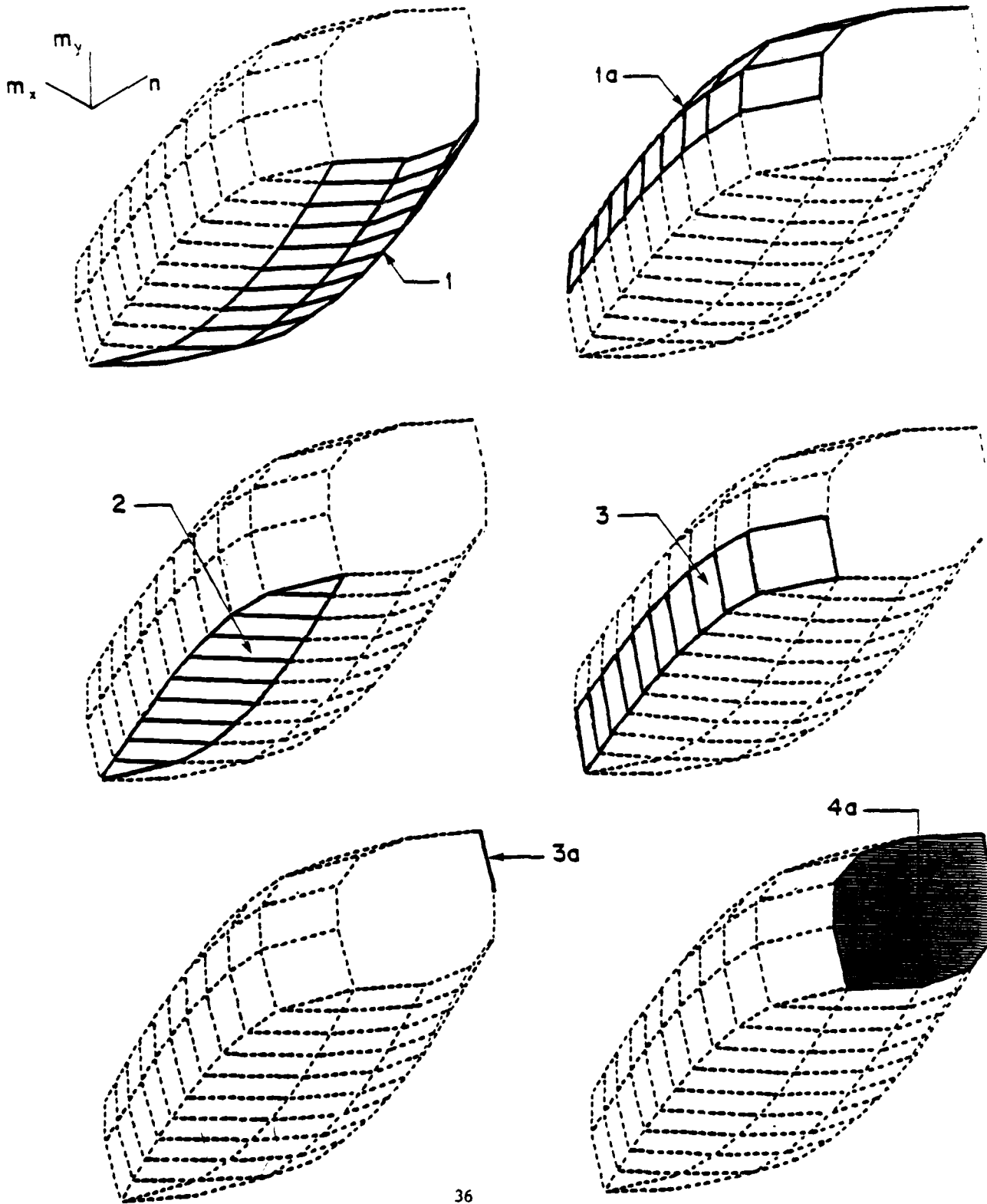


FIG. 13 Z SECTION YIELD SURFACE - $m_{\omega} = 0$

DISTRIBUTION LIST

DEPARTMENT OF DEFENSE

Assistant to the Secretary of Defense
Atomic Energy
ATTN: Executive Assistant

Defense Intelligence Agency
ATTN: DB-4C2
ATTN: DB-4C2, C. Wiehle
ATTN: DT-1C
ATTN: DT-2
ATTN: RTS-2A
ATTN: DB-4C3
ATTN: DB-4C, Rsch, Phys Vuln Br
ATTN: DB-4C1

Defense Nuclear Agency
ATTN: SPSS
ATTN: STSP
4 cy ATTN: TITL

Defense Technical Information Center
12 cy ATTN: DD

Field Command
Defense Nuclear Agency, Det 1
Lawrence Livermore Lab
ATTN: FC-1

Field Command
Defense Nuclear Agency
ATTN: FCPR
ATTN: FCT
ATTN: FCTX
ATTN: FCTT, G. Ganong
ATTN: FCTT, W. Summa
ATTN: FCTXE

Interservice Nuclear Weapons School
ATTN: TTV

Joint Strat Tgt Planning Staff
ATTN: NRI-STINFO Library
ATTN: JLA, Threat Applications Div
ATTN: JLTW, R. Autenberg
ATTN: JLTW-2
ATTN: DOXT
ATTN: XPFS

Under Secy of Def for Rsch & Engrg
ATTN: Strategic & Space Sys (OS)

DEPARTMENT OF THE ARMY

BMD Advanced Technology Center
ATTN: ICRDABH-X
ATTN: ATC-T

Chief of Engineers
ATTN: DAEN-RDL
ATTN: DAEN-MPE-T

Deputy Chief of Staff for Ops & Plans
ATTN: DAMO-NC, Nuc Chem Dir

Deputy Chief of Staff for Rsch Dev & Acq
ATTN: DAMA

DEPARTMENT OF THE ARMY (Continued)

Engineer Studies Center
ATTN: DAEN-FES, LTC Hatch

Harry Diamond Laboratories
ATTN: DELHD-NW-P
ATTN: DELHD-TA-L

US Army Concepts Analysis Agency
ATTN: CSSA-ADL

US Army Engineer Ctr & Ft Belvoir
ATTN: ATZA-DTE-ADM

US Army Engineer School
ATTN: ATZA, CDC

US Army Engr Waterways Exper Station
ATTN: R. Whalin
ATTN: WESSE
ATTN: WESSD, J. Jackson
ATTN: J. Strange
ATTN: J. Zelasko
ATTN: F. Brown
ATTN: Library
ATTN: WESSA, W. Flathau
ATTN: WESSS, J. Ballard

US Army Foreign Science & Tech Ctr
ATTN: DRXST-SD

US Army Mat Cmd Proj Mngr for Nuc Munitions
ATTN: DRCPM-NUC

US Army Material & Mechanics Rsch Ctr
ATTN: DRXMR, J. Mescall
ATTN: Technical Library

US Army Materiel Dev & Readiness Cmd
ATTN: DRCDE-D, L. Flynn
ATTN: DRXAM-TL

US Army Nuclear & Chemical Agency
ATTN: Library

US Army War College
ATTN: Library

USA Military Academy
ATTN: Document Library

DEPARTMENT OF THE NAVY

Marine Corp Dev & Education Command
ATTN: D091, J. Hartneady

Marine Corps
ATTN: POM

Naval Civil Engineering Laboratory
ATTN: Code L51, J. Crawford

Naval Coastal Systems Laboratory
ATTN: Code 741

DEPARTMENT OF THE NAVY (Continued)

David Taylor Naval Ship R&D Ctr
ATTN: Code L42-3
ATTN: Code 1700, W. Murray
ATTN: Code 1844
ATTN: Code 177, E. Palmer
ATTN: Code 172
ATTN: Code 1770.1
ATTN: Code 174
ATTN: Code 2740
ATTN: Code 1740.4
ATTN: Code 1740, R. Short
ATTN: Code 173
ATTN: Code 11
ATTN: Code 1740.5
ATTN: Code 1740.6
ATTN: Code 1740.1

Naval Electronic Systems Command
ATTN: PME 117-21

Naval Explosive Ord Disposal Fac
ATTN: Code 504, J. Petrousky

Naval Facilities Engineering Command
ATTN: Code 04B

Naval Material Command
ATTN: MAT 08T-22

Naval Ocean Systems Center
ATTN: Code 013, E. Cooper
ATTN: Code 4471

Naval Postgraduate School
ATTN: Code 69NE
ATTN: Code 1424, Library
ATTN: Code 69SG, Y. Shin

Naval Research Laboratory
ATTN: Code 8403, R. Belsham
ATTN: Code 8440, G. O'Hara
ATTN: Code 6380
ATTN: Code 8100
ATTN: Code 8301
ATTN: Code 8406
ATTN: Code 2627
ATTN: Code 8445
ATTN: Code 8404, H. Pusey

Naval Sea Systems Command
ATTN: SEA-033
ATTN: SEA-323
ATTN: SEA-06J, R. Lane
ATTN: SEA-09G53
ATTN: SEA-55X1
ATTN: SEA-08
ATTN: SEA-0351
ATTN: SEA-9931G

Naval Surface Weapons Center
ATTN: Code F34
ATTN: Code R13
ATTN: Code R10
ATTN: Code U401, M. Kleinerman
ATTN: Code R14
ATTN: Code F31
ATTN: Code R15

DEPARTMENT OF THE NAVY (Continued)

Naval Surface Weapons Center
ATTN: W. Wishard
ATTN: Tech Library & Info Svcs Br

Naval War College
ATTN: Code E-11

Naval Weapons Center
ATTN: Code 233
ATTN: Code 266, C. Austin
ATTN: Code 3263, J. Bowen

Naval Weapons Evaluation Facility
ATTN: G. Binns
ATTN: Code 10
ATTN: Code 210
ATTN: R. Hughes

Naval Weapons Support Center
ATTN: Code 70553, D. Moore

New London Laboratory
ATTN: Code 4494, J. Patel
ATTN: Code 4492, J. Kalinowski

Newport Laboratory
ATTN: Code EM
ATTN: Code 363, P. Paranzino

Ofc of the Deputy Chief of Naval Ops
ATTN: OP 987
ATTN: NOP 982, Tac Air Srf & Ewdev Div
ATTN: NOP 981
ATTN: NOP 654, Strat Eval & Anal Br
ATTN: OP 098T8
ATTN: OP 982E, M. Lenzini
ATTN: OP 957E
ATTN: NOP 953, Tac Readiness Div
ATTN: OP 37
ATTN: OP 225
ATTN: OP 03EG
ATTN: OP 21
ATTN: NOP 951, ASW Div
ATTN: OP 605D5
ATTN: OP 981N1
ATTN: OP 223

Office of Naval Research
ATTN: Code 474, N. Perrone

Strategic Systems Project Office
ATTN: NSP-272
ATTN: NSP-43
ATTN: NSP-273

DEPARTMENT OF THE AIR FORCE

Air Force Institute of Technology
ATTN: Commander
ATTN: Library

Air Force Systems Command
ATTN: DLW

Assistant Chief of Staff
Intelligence
ATTN: IN

DEPARTMENT OF THE AIR FORCE (Continued)

Air Force Weapons Laboratory
ATTN: NTEG-G, S. Melzer
ATTN: NTE, M. Plamondon
ATTN: NTEG-C, R. Henny
ATTN: SUL
ATTN: NTEG

Ballistic Missile Office
ATTN: DEB

Deputy Chief of Staff
Research, Development, & Acq
ATTN: AFRDQI
ATTN: R. Steere

Deputy Chief of Staff
Logistics & Engineering
ATTN: LEEB

Foreign Technology Division
ATTN: NIIS Library
ATTN: TQTD
ATTN: SDBG
ATTN: SDBF, S. Spring

Rome Air Development Center
ATTN: RBES, R. Mair
ATTN: Commander
ATTN: TSLD

Strategic Air Command
ATTN: NRI-STINFO Library

DEPARTMENT OF ENERGY

Albuquerque Operations Office
ATTN: CTID

Department of Energy
ATTN: OMA/RD&T

Nevada Operations Office
ATTN: Doc Con for Technical Library

OTHER GOVERNMENT AGENCIES

Central Intelligence Agency
ATTN: OSWR/NED
ATTN: OSR/SE/F

NASA
ATTN: F. Nichols
ATTN: R. Jackson

NATO

NATO School
SHAPE
ATTN: US Documents Officer

DEPARTMENT OF ENERGY CONTRACTORS

University of California
Lawrence Livermore National Lab
ATTN: S. Erickson

DEPARTMENT OF ENERGY CONTRACTORS (Continued)

Los Alamos National Laboratory
ATTN: R. Whitaker
ATTN: MS530, G. Spillman
ATTN: Reports Library
ATTN: MS634, T. Dowler
ATTN: R. Sanford
ATTN: MS670, J. Hopkins

DEPARTMENT OF DEFENSE CONTRACTORS

Applied Research Associates, Inc
ATTN: D. Piepenburg

Applied Research Associates, Inc
ATTN: B. Frank

BDM Corp
ATTN: T. Neighbors
ATTN: A. Lavagnino
ATTN: Corporate Library

California Institute of Technology
ATTN: T. Ahrens

California Research & Technology, Inc
ATTN: M. Rosenblatt
ATTN: S. Schuster
ATTN: Library
ATTN: K. Kreyenhagen

Columbia University
ATTN: H. Bleich
ATTN: F. Dimaggio

University of Denver
ATTN: Sec Officer for J. Wisotski

Electric Power Research Institute
ATTN: G. Sliter

Electro-Mech Systems, Inc
ATTN: R. Shunk

General Dynamics Corp
ATTN: J. Miller
ATTN: J. Mador
ATTN: M. Pakstys

Kaman Avidyne
ATTN: R. Ruetenik
ATTN: G. Zartarian
ATTN: Library
ATTN: N. Hobbs

Kaman Sciences Corp
ATTN: Library
ATTN: F. Shelton

Kaman Sciences Corp
ATTN: D. Sachs

Kaman Tempo
ATTN: DASIAC

DEPARTMENT OF DEFENSE CONTRACTORS (Continued)

Karagozian and Case
ATTN: J. Karagozian

Lockheed Missiles & Space Co, Inc
ATTN: Technical Information Center
ATTN: T. Geers
ATTN: B. Almroth

Lockheed Missiles & Space Co, Inc
ATTN: TIC-Library

M & T Company
ATTN: D. McNaught

Management Science Associates
ATTN: K. Kaplan

McDonnell Douglas Corp
ATTN: R. Halprin

NKF Engineering Associates, Inc
ATTN: R. Belsheim

Pacific-Sierra Research Corp
ATTN: H. Brode, Chairman SAGE

Pacifica Technology
ATTN: R. Bjork
ATTN: G. Kent
ATTN: A. Kushner

Physics Applications, Inc
ATTN: C. Vincent

Physics International Co
ATTN: L. Behrmann
ATTN: F. Sauer
ATTN: J. Thomsen
ATTN: E. Moore
ATTN: Technical Library

Science Applications, Inc
ATTN: Technical Library

Southwest Research Institute
ATTN: A. Wenzel
ATTN: W. Baker

DEPARTMENT OF DEFENSE CONTRACTORS (Continued)

S-CUBED
ATTN: T. Cherry
ATTN: R. Sedgewick
ATTN: D. Grine
ATTN: T. Riney
ATTN: Library
ATTN: K. Pyatt
ATTN: T. McKinley

SRI International
ATTN: G. Abrahamson
ATTN: W. Wilkinson
ATTN: A. Florence

Teledyne Brown Engineering
ATTN: J. Ravenscraft

Tetra Tech, Inc
ATTN: L. Hwang

TRW Electronics & Defense Sector
ATTN: P. Bhuta
ATTN: A. Feldman
ATTN: N. Lipner
ATTN: Technical Information Center
ATTN: D. Jortner
ATTN: B. Sussholtz

TRW Electronics & Defense Sector
ATTN: P. Dai
ATTN: F. Pieper
ATTN: E. Wong
ATTN: G. Hulcher

Weidlinger Assoc, Consulting Engrg
ATTN: J. McCormick
ATTN: M. Baron
4 cy ATTN: R. Daddazio
4 cy ATTN: M. Bieniek
4 cy ATTN: F. Dimaggio

Weidlinger Associates
ATTN: J. Isenberg

DATE
ILME